iScience

CellPress
OPEN ACCESS

Article

Accurate and stable chronic *in vivo* voltammetry enabled by a replaceable subcutaneous reference electrode

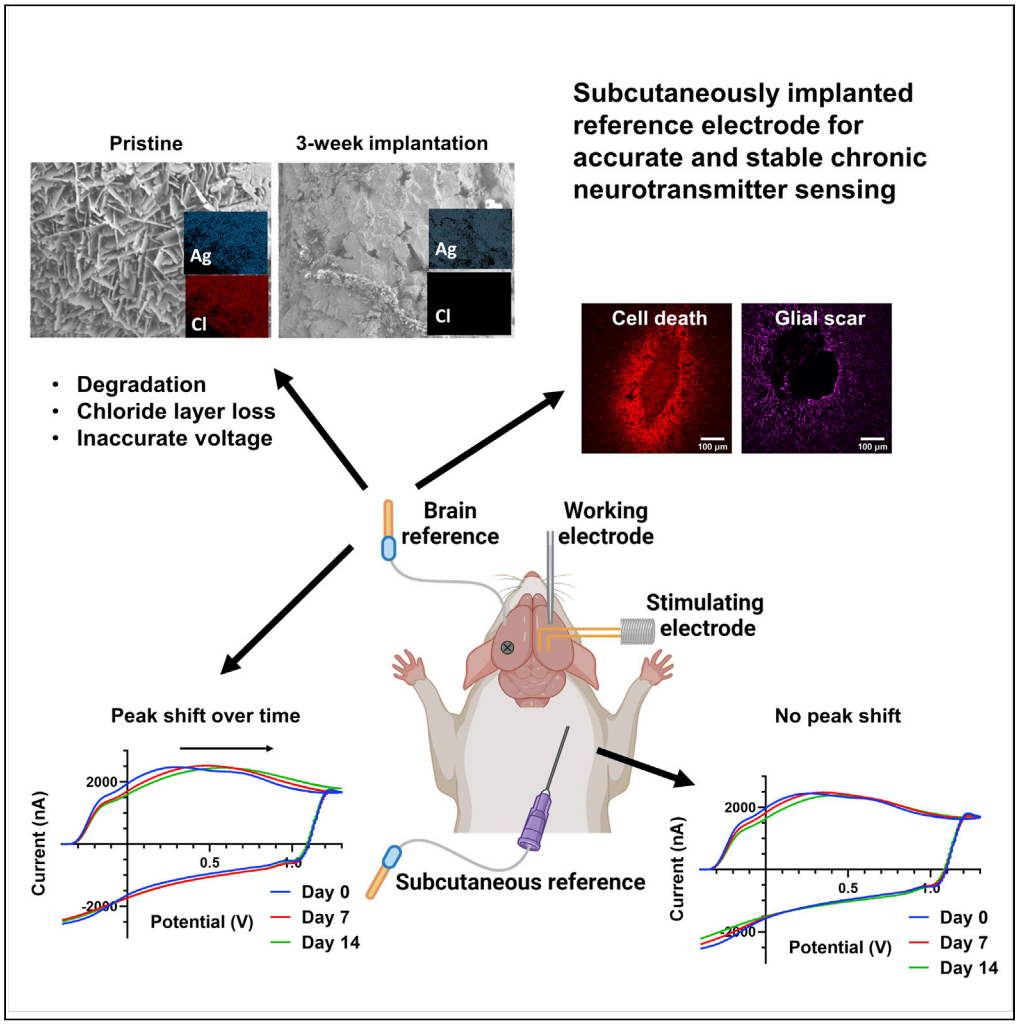

Elaine Marie Robbins, Elisa Castagnola, Xinyan Tracy Cui

xic11@pitt.edu

Highlights

Chronic reference electrodes in the brain degrade, resulting in inaccurate voltages

Implantation also causes substantial tissue damage and cell death

A replaceable subcutaneous reference enables more accurate chronic measurements

Brain tissue damage is also eliminated with a subcutaneous reference

Robbins et al., iScience *25*, 104845
August 19, 2022
https://doi.org/10.1016/j.isci.2022.104845

iScience

CellPress
OPEN ACCESS

Article

Accurate and stable chronic *in vivo* voltammetry enabled by a replaceable subcutaneous reference electrode

Elaine Marie Robbins,[1] Elisa Castagnola,[1] and Xinyan Tracy Cui[1,2,3,4,*]

SUMMARY

***In vivo* sensing of neurotransmitters has provided valuable insight into both healthy and diseased brain. However, chronically implanted Ag/AgCl reference electrodes suffer from degradationgradation, resulting in errors in the potential at the working electrode. Here, we report a simple, effective way to protect *in vivo* sensing measurements from reference polarization with a replaceable subcutaneously implanted reference. We compared a brain-implanted reference and a subcutaneous reference and observed no difference in impedance or dopamine redox peak separation in an acute preparation. Chronically, peak background potential and dopamine oxidation potential shifts were eliminated for three weeks. Scanning electron microscopy shows changes in surface morphology and composition of chronically implanted Ag/AgCl electrodes, and postmortem histology reveals extensive cell death and gliosis in the surrounding tissue. As accurate reference potentials are critical to *in vivo* electrochemistry applications, this simple technique can improve a wide and diverse assortment of *in vivo* preparations.**

INTRODUCTION

Fast scan cyclic voltammetry (FSCV) is an electrochemical detection technique that has been utilized extensively for decades for neurochemical sensing *in vivo* (Puthongkham and Venton, 2020). FSCV has been used to detect dopamine (DA) (Heien et al., 2003; Hoffman et al., 2016; Phillips et al., 2003; Taylor et al., 2017b; Walters et al., 2015, 2016), serotonin (Hashemi et al., 2011a; Saylor et al., 2019; West et al., 2019), histamine (Hashemi et al., 2011a; Puthongkham et al., 2019;Samaranayake et al., 2015, 2016), adenosine (Borgus et al., 2020; Ross and Venton, 2014; Swamy and Venton, 2007; Wang and Venton, 2019), hydrogen peroxide (Sanford et al., 2010; Wilson et al., 2018), pH (Heien et al., 2005), oxygen (Wang and Venton, 2019), and melatonin (Castagnola et al., 2020a; Hensley et al., 2018), among other compounds. FSCV exploits several electrochemical properties of microelectrodes to isolate the faradaic current resulting from the redox reaction of an analyte as a means of chemical sensing *in vivo* (Aoki, 1993; Bard and Faulkner, 2001). As a result of the high scan rates employed in this technique, a large capacitive current is generated that must be subtracted out to isolate the faradaic current resulting from the reaction of interest. Therefore, FSCV relies heavily on a highly stable background that can be subtracted from data recorded during a change in analyte concentration resulting from stimulation (George et al., 2021; Taylor et al., 2012), drug (Phillips et al., 2003; Siciliano et al., 2018), or behavior (Heien et al., 2005; Moran et al., 2018).

FSCV has found extensive use in chronic and behaving applications (Montague et al., 2004). Behavioral studies in awake animals have provided insights into addiction and reward mechanisms (Heien et al., 2005; Howe et al., 2013; Owesson-White et al., 2016; Park et al., 2015; Phillips et al., 2003). Additionally, carbon fiber arrays are advancing as a method for performing FSCV at multiple locations simultaneously over long periods of time (Patel et al., 2015, 2016, 2020; Welle et al., 2021; Schwerdt et al., 2017a, 2017b). Chronic FSCV is difficult due to biofouling of both the carbon fiber working electrode and the reference electrode. Several strategies have been explored to protect the carbon fiber electrode from fouling, including antifouling coatings (Zhou et al., 2019), surface optimizations (Weese et al., 2019), and electrochemical surface renewal (Rafi and Zestos, 2021). The reference electrode, typically Ag wires coated with AgCl that are cemented in place during the duration of the experiment, has been less explored.

[1]Department of Bioengineering, University of Pittsburgh, 5057 Biomedical Science Tower 3, 3501 Fifth Avenue, Pittsburgh, PA 15260, USA

[2]Center for Neural Basis of Cognition, Pittsburgh, PA, USA

[3]McGowan Institute for Regenerative Medicine, Pittsburgh, PA, USA

[4]Lead contact

*Correspondence: xic11@pitt.edu

https://doi.org/10.1016/j.isci.2022.104845

It is well known that chronic FSCV measurement quality suffers over time due to polarization of the reference electrode; meaning, the reference electrode's potential will change upon passage of current and no longer behaves as an ideal nonpolarizable electrode in the desired potential range. Over time, the faradaic and non-faradaic current will change because of de-chlorination (i.e., dissolution of the AgCl layer (Suzuki et al., 1998)) and biofouling at the surface of the Ag/AgCl wire that affects the potential at the working electrode (Seaton et al., 2020). This can complicate background subtraction and cause difficulty in identifying voltammograms as the analyte of interest. Other controlled potential electrochemical techniques for neurochemical sensing like multiple cyclic square wave voltammetry also frequently use brain-implanted Ag/AgCl wires as references and are likely affected by biofouling-induced polarization (Yuen et al., 2021).

Several strategies have been proposed to minimize reference polarization. For example, Seaton et al. recently showed that using a 3-electrode configuration *in vivo* with a Pt counter electrode and Ag/AgCl reference can compensate for biofouling-induced electrochemical impedance increases *in vivo* and may preserve the long-term DA sensitivity (Seaton et al., 2020). Additionally, Nafion and polyurethane coatings have been shown to preserve the Ag/AgCl reference electrode integrity for up to 28 days (Hashemi et al., 2011b; Moatti-Sirat et al., 1992; Moussy and Harrison, 1994; Wang et al., 2019). Regardless of two or three electrode set up, Ag and AgCl may present brain toxicity; extensive tissue damage and behavioral abnormalities have been found in animals and humans implanted with Ag or Ag/AgCl electrodes (Cooper and Crow, 1966; Jackson and Duling, 1983; Li et al., 2009).

To combat reference electrode polarization and Ag-induced tissue damage, we introduce here an alternative to the permanently brain-implanted Ag wires typically used for chronic and behaving FSCV measurements. We report a simple method to improve FSCV data quality using a removable Ag wire electrode inserted subcutaneously in the rat. By utilizing a new reference electrode during every recording session, biofouling-induced polarization is not an issue. In addition, the Ag wire is kept out of the brain, preventing damage and tissue death resulting from both the electrode implantation and the highly toxic Ag itself. This has the potential to improve the quality of data recorded from behaving animals.

Upon implantation, we observed no difference in background current or impedance when comparing a traditional brain-implanted Ag/AgCl reference and a reference electrode inserted subcutaneously on the back of a rat. We detected stimulated DA release using both electrode schemes and determined no difference in the peak separation or oxidation potential of DA, indicating that a subcutaneous reference wire is a viable alternative. In addition, we chronically implanted a carbon fiber microelectrode and performed FSCV experiments over a period of two weeks, using a Ag/AgCl reference electrode chronically implanted in the brain vs. acutely inserted subcutaneously on each day of FSCV measurement. We found that the background shift observed with the chronically implanted reference was eliminated by using the subcutaneous reference. This also held true for DA transients detected in an awake head-fixed mouse after 3 weeks of implantation. Additionally, we investigated utilizing a third electrode to divert the current flow through a bone screw counter electrode, rather than the reference electrode. We found that operating in a 3-electrode configuration does not mitigate the effects of reference electrode polarization *in vivo*. Scanning electron microscopy (SEM) and energy-dispersive X-ray spectroscopy (EDX) revealed that while there was little tissue adhered to the surface of the explanted electrodes, they no longer had a Cl-containing layer on the surface. Histology reveals severe tissue damage at the location of the brain-implanted reference, indicating that a reference electrode implanted outside of the brain would be ideal for chemical measurements coupled to behavioral observations.

RESULTS

Subcutaneously implanted reference electrode can be used for controlled potential experiments

We investigated whether Ag/AgCl wires implanted subcutaneously into the fat on the back of anesthetized rats can be used for potentiostatic experiments. A schematic of the experimental setup is presented in Figure 1A. We performed electrochemical impedance spectroscopy measurements at a carbon fiber working electrode, using either a brain-implanted reference or a subcutaneously implanted one. Impedance measurements of a carbon fiber electrode using either a standard brain-implanted Ag wire or the subcutaneously implanted wire are indistinguishable in n = 5 rats (Figure 1B). Additionally, the background current generated by scanning the FSCV waveform using either the brain-implanted reference or subcutaneous

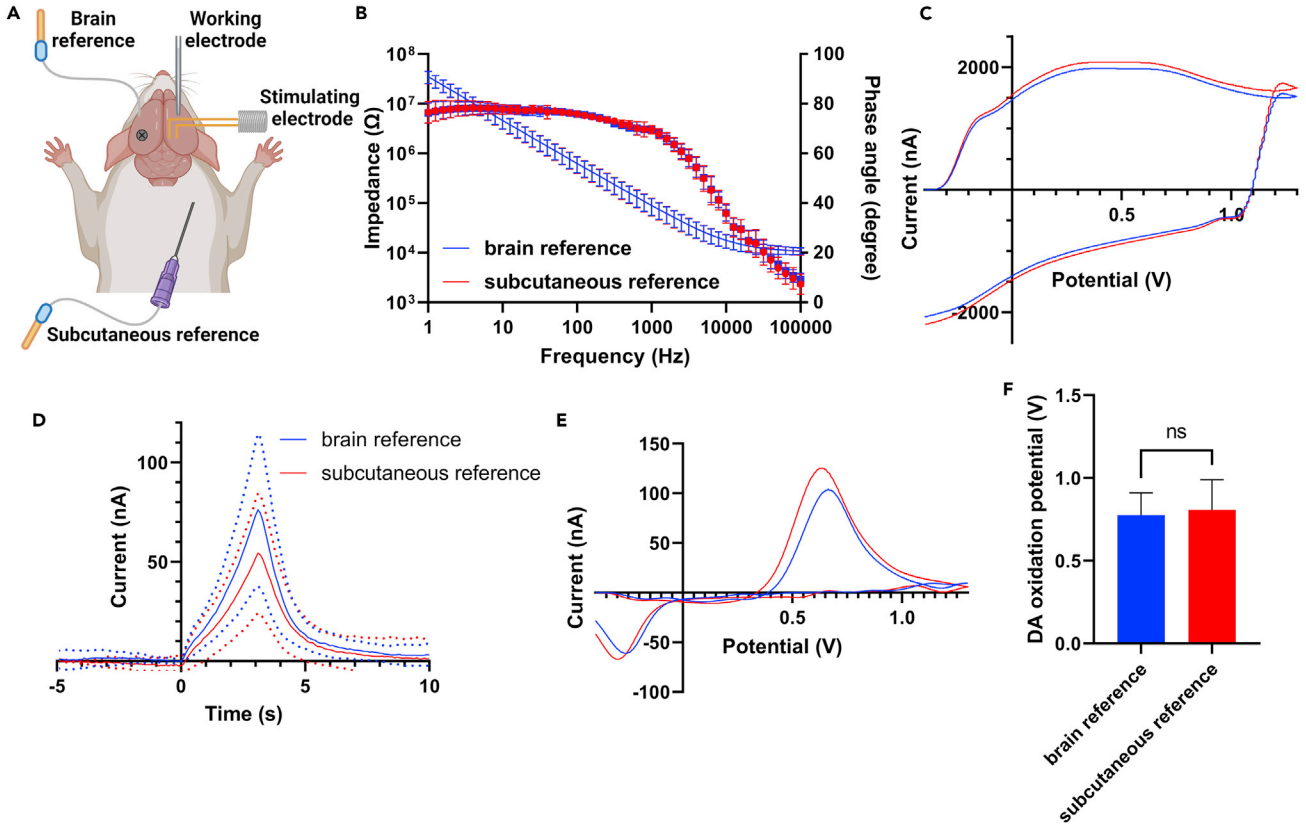

Figure 1. Subcutaneously implanted reference electrodes can be used for FSCV

(A) Schematic of the experimental setup. The carbon fiber working electrode in the striatum was used to detect dopamine released by the stimulating electrode in the medial forebrain bundle. Measurements were made with either a brain-implanted Ag/AgCl electrode, or a subcutaneously inserted Ag/AgCl electrode. The subcutaneous electrode was inserted with the aid of a needle guide.

(B) The impedance (blue) and phase angle (red) (n = 5, mean ± SD) of the carbon fiber working electrode taken vs the reference implanted into the brain (circles) and the subcutaneous reference (triangles) immediately after implantation.

(C) The total current detected (faradaic and non-faradaic) at the working electrode when using the brain reference (blue) or the subcutaneous reference (red) in two-electrode mode to scan the FSCV waveform. Mean of n = 5 rats, SDs omitted for clarity.

(D) In an acute preparation, the observed stimulated DA in response to a 60 Hz 180 pulse stimulation is not significantly different when using either a brain-implanted reference (blue) or a subcutaneously implanted reference (red) (mean ± SD, n = 5 rats, three repetitions).

(E) The response to subsequent stimulations in one animal using either the brain reference (blue) or the subcutaneous reference (red) is similar.

(F) The oxidation potential of DA is also not significantly different between the brain or subcutaneous reference electrode (mean ± SD, unpaired t tet, ns, no significance).

reference was similar (Figure 1C); the position of the reference electrode does not affect the potential at the working electrode and ability of the electric double layer to charge and discharge.

Upon electrical stimulation of the MFB, the carbon fiber electrode in the striatum detected DA overflow using either the brain reference or the subcutaneous reference. The temporal dynamics of the observed responses were similar (Figure 1D). The background-subtracted CV at the maximum current level is a characteristic DA CV in both cases (Figure 1E). Interrogation of the oxidation potential of DA (Figure 1F) reveals no significant difference between the brain reference and subcutaneous reference for either parameter. Using an Ag/AgCl reference electrode placed subcutaneously rather than implanted directly into the brain tissue seems to have no effect on the ability to detect DA release evoked by electrical stimulation and the potential of the working electrode. Therefore, a subcutaneous reference is a viable alternative to a brain-implanted reference electrode.

Using a subcutaneous, replaceable reference prevents background shifting over time

The most useful potential application of this reference electrode placement is in the case of chronic implants, where reference electrode degradation and biofouling may alter the effective potential at the

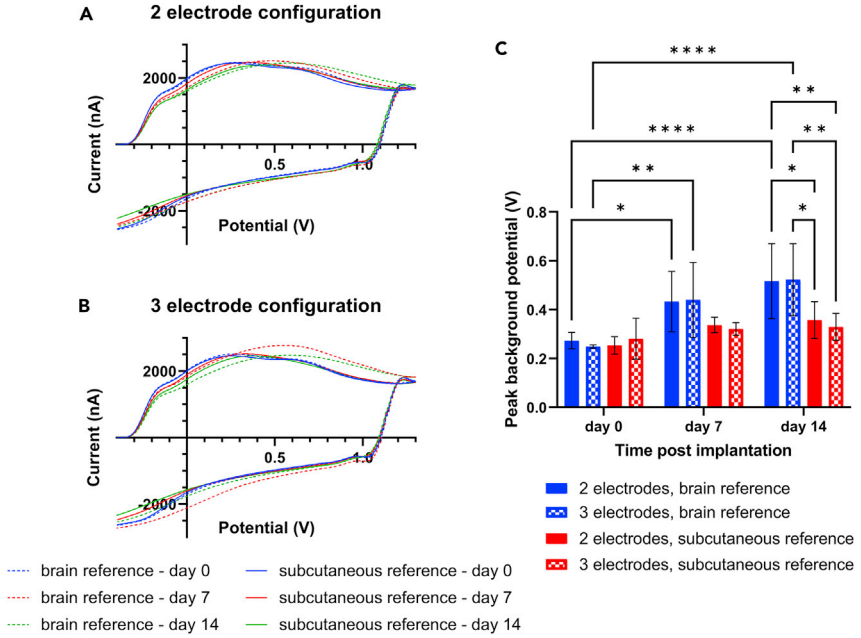

Figure 2. Mean changes in the total non-background-subtracted current measured over time in 2-electrode configuration and in 3-electrode configuration

A new, pristine subcutaneous reference electrode was used for each experimental session (n = 3 rats, three repetitions), while the brain reference and working electrode were chronically implanted for the duration of the time frame. The number of days post implantation refers to the chronic brain reference and working electrodes. (A) Using the brain-implanted reference, on day 7 and 14 there was a shift in the peak potential of the background current in 2-electrode mode (red and green dashed lines, respectively). This change is not observed using the subcutaneously implanted reference electrode (solid lines).

(B) In 3-electrode configuration, a shift in the peak potential of the background current is still observed using the brain-implanted reference on day 7 (red, dashed line) and day 14 (green, dashed line), but not in the subcutaneous reference (solid lines).

(C) Mean ± SD of the potential where the peak background current is observed using the brain-implanted reference in 2-electrode mode (blue solid bars) and 3-electrode mode (blue checked bars), and for the subcutaneous reference in 2-electrode mode (red solid bars) and 3-electrode mode (red checked bars).

A significant shift at each timepoint when using the brain reference regardless of electrode configuration. No significant shift is seen when using the subcutaneous reference. (two-way ANOVA, multiple comparisons, * = $p < 0.05$, ** = $p < 0.005$, **** = $p < 0.00005$).

working electrode, resulting in a background shift, and therefore a shift in an analyte's observed peak redox potential. To investigate this, we chronically implanted carbon fiber electrodes and Ag/AgCl wires into the brains of n = 3 rats and took weekly FSCV measurements. Additionally, FSCV measurements were also taken using a pristine Ag/AgCl electrode implanted subcutaneously immediately prior to the measurements. In both cases, the measurements were taken in either 2-electrode mode (where the counter and reference are shorted at the Ag/AgCl electrode) or in 3-electrode mode using a bone screw counter electrode.

In a 2-electrode configuration with a reference electrode implanted in the brain, which is typical for chronic *in vivo* FSCV experiments, background current will shift over time partly due to reference electrode fouling (Seaton et al., 2020). We also observed this shift; each week the peak oxidative background potential (maximum potential in the background CV) increased, as shown in Figure 2A, and quantified in Figure 2C. In a 3-electrode configuration, no current flows through the reference electrode—all the current flow is through the counter electrode, in this case a bone screw (Bard and Faulkner, 2001). 3-electrode configuration is rarely used for FSCV as a third electrode not typically necessary due to the small currents involved. Using a 3-electrode setup is also more hazardous, as it presents a potential shock risk to the animal and damage to the working electrode that is eliminated by a 2-electrode configuration. In our hands, 3-electrode configuration did not aid in preventing background potential change over time (Figures 2B

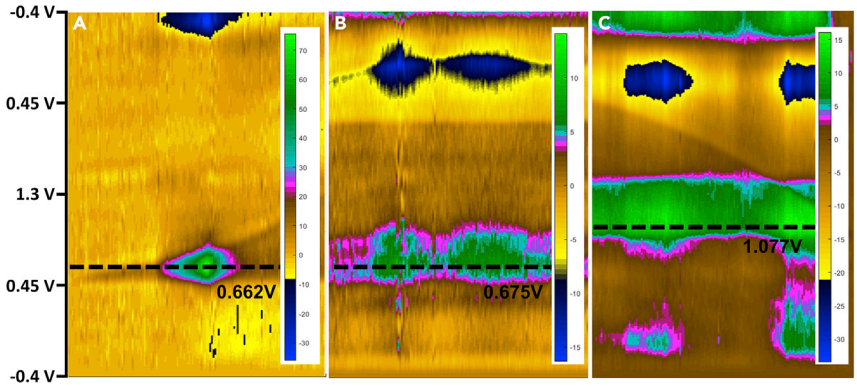

Figure 3. DA peak oxidation potential shift is eliminated with a subcutaneous reference

(A–C) (A) Colorplot of electrically evoked DA detected using a fresh brain-implanted Ag/AgCl reference electrode, used as a baseline to determine the DA oxidation potential in an ideal *in vivo* scenario. After 3 weeks of carbon fiber and brain reference implantation, spontaneous transient DA signals were detected in an awake head-fixed mouse using either a fresh, subcutaneous reference (B) or the chronically implanted brain reference (C). Each colorplot represents 15 s of FSCV recording. The dashed line represents the potential at which the maximum oxidation current was detected.

and 2C). However, in both 2- and 3-electrode configuration, a newly implanted subcutaneous reference electrode was able to prevent peak background potential shift.

A subcutaneous reference prevents dopamine oxidation peak shifts over time for three weeks

To test whether the subcutaneous reference can be used to detect DA in a chronic application, a mouse was implanted with a reference electrode and a carbon fiber electrode in the striatum. Additionally, a stainless-steel frame was cemented in place. After 3 weeks of implantation, the mouse was briefly re-anesthetized, a subcutaneous reference was inserted under the skin, and the mouse was placed on a treadmill. The anesthesia was then discontinued, and FSCV recordings of spontaneous DA transients were taken in the awake, head-fixed mouse. As in the anesthetized rats, the peak oxidative background potential in the brain reference was shifted positively by 140 mV compared to the subcutaneous reference. Compared to evoked DA detected at a newly implanted carbon fiber electrode with a fresh brain-implanted Ag/AgCl reference (Figure 3A), DA transients detected after 3 weeks of working electrode implantation with a new subcutaneous reference have a very similar oxidation potential (Figure 3B). However, DA transients detected with the 3 weeks chronically implanted brain reference have a significant shift in oxidation potential (Figure 3C). This shift means that we can only tentatively identify this current as DA oxidation.

SEM/EDX analysis of explanted electrodes reveals loss of the AgCl layer

After 3 weeks of electrode implantation, rats were sacrificed and perfused and their brains were removed. Explanted Ag/AgCl electrodes were analyzed using SEM/EDX to determine surface Cl content compared to a freshly prepared Ag/AgCl electrode. The pristine Ag/AgCl electrodes have a distinct surface structure with a fairly uniform distribution of Ag and Cl (Figure 4A, Ag and Cl map in inset). However, the explanted Ag/AgCl electrodes have a much smoother morphology (Figures 4B–4D). Electrodes explanted after 1, 2, or 3 of implantation in the brain show progressive loss of the Cl layer. Small amounts of AgCl remain in the 1- and 2-week implanted electrodes (insets of Figures 4B and 4C), but by 3 weeks of implantation the AgCl layer is almost completely gone (Figure 4D). Multiple sites of multiple electrodes show that explanted electrodes contain very little Cl compared to the Ag doublet at 3-3.2 keV. Representative spectra are shown in Figures 4E and 4F. Compared to the pristine electrode in Figures 4E and 4D, the Cl peak at 2.7 keV is greatly diminished in the electrode implanted for 3 weeks in Figure 4F. While we observed some tissue adherence to one explanted electrode, most of the surfaces analyzed were relatively free of tissue.

Ag/AgCl reference electrodes implanted in the brain cause severe tissue damage

We performed immunohistological staining to investigate the tissue damage around the brain-implanted reference electrode after 1, 2, or 3 weeks of electrode implantation. NeuN staining (Figure 5B) reveals a

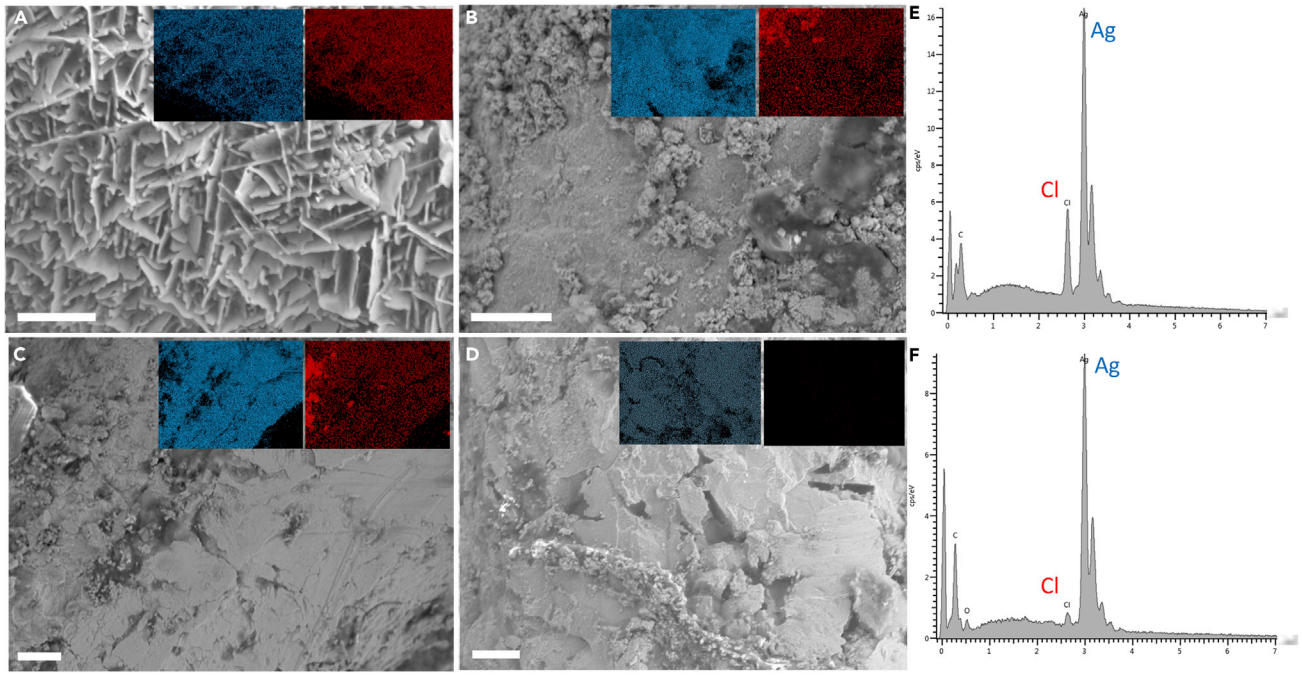

Figure 4. SEM/EDX analysis of Ag/AgCl electrodes, all prepared with the same procedure

(A–D) Scale bar = 10 μm (A) SEM image of a freshly prepared Ag/AgCl electrode. The inset shows an EDX map of the distribution of Ag (blue) and Cl (red).

(B–D) SEM image of Ag/AgCl reference electrodes after 1 (B), 2 (C), or 3 (D) weeks of implantation. The insets show a EDX maps of the distribution of Ag and Cl.

(E) EDX spectrum of a freshly prepared Ag/AgCl electrode.

(F) EDX spectrum of a tissue-free area of a Ag/AgCl electrode after 3 weeks of implantation.

severe depletion of neurons around the electrode track at all 3 weeks. Caspase-3, a marker of apoptosis, is highly expressed in the area surrounding the electrode track, increasing over time (Figure 5B). While tissue death is unlikely to affect reference electrode polarization, which is most likely due to Ag/AgCl de-chlorination (Rodeberg et al., 2017), it is an undesirable outcome. Ag wires directly implanted into the brain (rather than the electrical connection being made through a salt bridge) are commonly employed in the cases of chronic and behavioral-controlled potential measurements. In these cases, tissue damage even distal to the working electrode can affect the animal's response to behavioral tasks. Similarly, GFAP expression increases over time (Figure 5D). At week 1 (top row), processes are extended toward the implant, and by week 3 (bottom row) a mature glial barrier has begun to form, in agreement with another assessment of Ag/AgCl electrode immunohistochemistry (Hashemi et al., 2011b). Iba-1 expression (Figure 5E) shows significant microglia activation in the first week after implantation that decreases over the following weeks.

DISCUSSION

Ag/AgCl is used commonly for *in vivo* studies because of its simple construction and electrochemical properties (Kahlert, 2010). Ag/AgCl electrodes approach the behavior of an ideal nonpolarizable electrode in current ranges relevant to a typical *in vivo* sensor experiment at a small electrode, meaning that the current passing through the reference electrode will not induce a change in potential. The AgCl layer acts as the depolarizer—it causes the potential of the electrode to approach its equilibrium value by being oxidized or reduced at the electrode surface (Bard and Faulkner, 2001). AgCl has non-negligible solubility, even *in vitro* in concentrated KCl solutions (Suzuki et al., 1998). When the depolarizing layer is gone, the reference electrode loses its nonpolarizable character. EDX revealed that in addition to gross surface morphology changes, the explanted electrodes had a negligible amount of Cl left on their surface, indicating that the electrodes were now polarizable and not suitable as a reference electrode.

We demonstrate here that placing a reference electrode outside of the brain is a viable option for several different types of *in vivo* electrochemical experiments. Potentiostatic measurements (FSCV) were performed using a subcutaneous reference electrode. There was no significant difference between FSCV

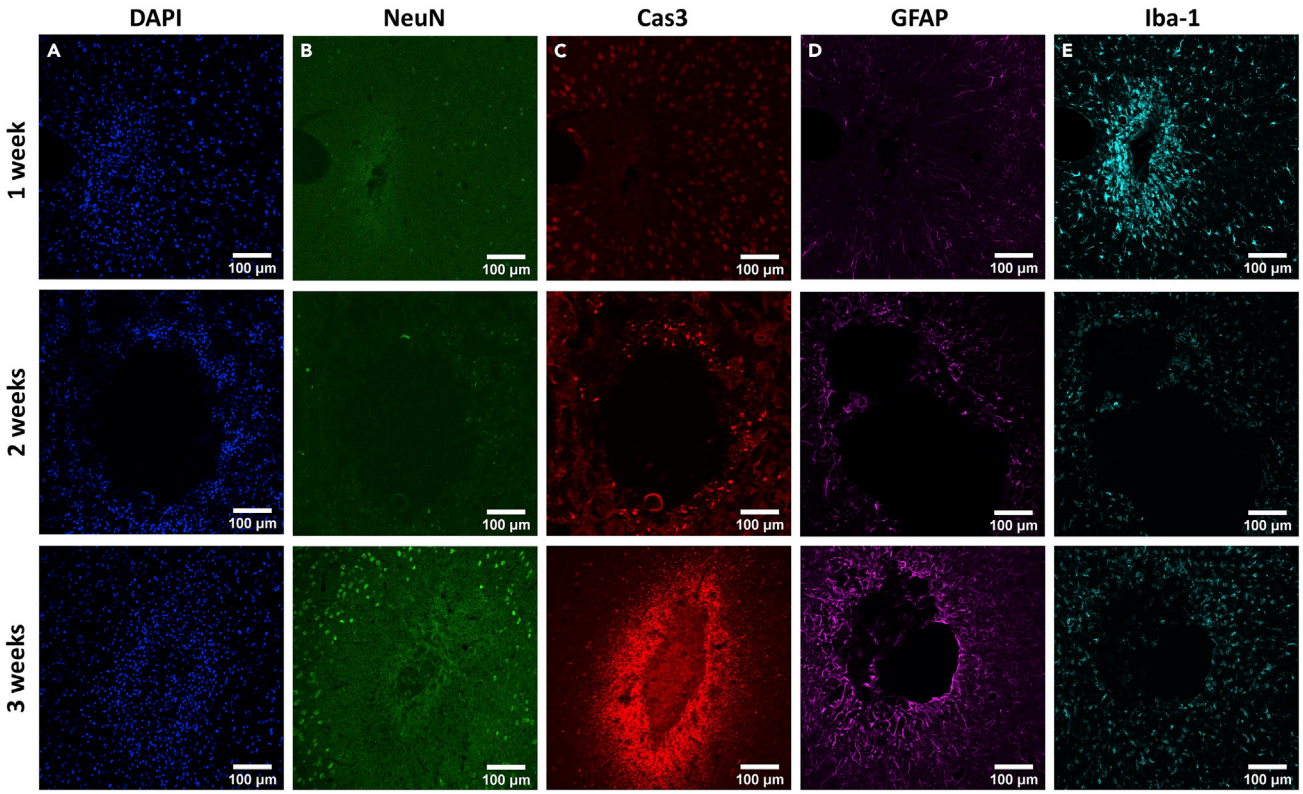

Figure 5. Histological analysis of the tissue surrounding the Ag/AgCl electrode

(A–E) Images of Ag/AgCl reference electrode tracks in the brain after 1 (top row), 2 (middle row), or 3 (bottom row weeks of implantation stained for (A) DAPI (blue) (B) NeuN (green), (C) caspase-3 (red), (D) GFAP (magenta), and (E) Iba-1 (cyan). There is significant and increasing caspase-3 activation and profound neuron death around the electrode track, as well as increasing GFAP activity over the course of 3 weeks and immediate microglia activation.

background current measured in rats using either the brain-implanted reference or the subcutaneous reference. The background-subtracted CVs of DA evoked via electrical stimulation also showed identical oxidation potential and peak separation with the two references. Additionally, spontaneous transients detected in an awake, head-fixed mouse showed a significant shift when using the 3-week chronically implanted brain reference, compared to a fresh subcutaneous reference. Therefore, there is no change in the ability of the carbon fiber working electrode to charge and discharge its electric double layer and oxidize and reduce electrochemical species when the reference electrode is placed outside of the brain. This technique can be applied to improve the reliability of potential control techniques for not only FSCV but also other electrochemical sensing studies (Atcherley et al., 2013; He et al., 2020; Park et al., 2018; Taylor et al., 2017a; Wassum et al., 2008; Yuen et al., 2021), voltage-controlled drug delivery (Weaver et al., 2014), and voltage transient measurements in chronic stimulation studies (Merrill et al., 2005; Zheng et al., 2020, 2021).

While all controlled potential techniques rely on a stable reference potential and are also likely affected by reference electrode polarization that can be eliminated with this technique, FSCV is uniquely vulnerable due to the necessity of a stable background current. Shifts in background potential are a well-known issue with chronic FSCV (Rodeberg et al., 2017). Over time, the peak of the background current will shift to a more positive potential. This shift is identified to be a result of reference electrode fouling and is indicative of an error in the voltage applied to the working electrode. This shift may confound the identification of DA, as its characteristic oxidation and reduction potentials will also shift. This also presents an issue for principal component analysis, which relies on a very stable, reproducible background current. Shifting background currents will hinder the accurate identification of the DA principal component. While reference electrode fouling can be dampened with the use of polymer coatings like Nafion and polyurethane (Hashemi et al., 2011b; Moussy and Harrison, 1994), the effects of these coatings on the toxicity of the Ag wire have not been investigated.

In our experimental setup, we were not able to prevent background potential shift by switching to a 3-electrode configuration with the brain-implanted reference. This result is contrary to a recent report from Seaton et al. that operating in a 3-electrode configuration can prevent background shift because current is passed through the low-impedance counter electrode rather than a potentially fouled high-impedance Ag/AgCl wire (Seaton et al., 2020). They observed significant biofouling of explanted electrodes, with substantial buildup of tissue-derived material on the surface. Typically, FSCV is performed with two electrodes because IR drop is minimal due to the low currents, and due to the inherent shock hazard of a 3-electrode setup. Increased reference electrode impedance may result in a more significant IR drop in a 2-electrode cell due to the increased solution resistance (Bard and Faulkner, 2001; Heinze, 1993). Equation (1) defines the relationship between the applied potential, the potential at the working electrode, and IR drop:

$$E_{app} = E_{working} + IR_S \quad \text{(Equation 1)}$$

where E_{app} is the potential being applied by the potentiostat, $E_{working}$ is the potential of the working electrode (both vs. Ag/AgCl), I is the current flow between the working and reference electrodes, and R_S is the solution resistance between the working and reference electrodes. As the IR_S term increases with increased gliosis-induced solution resistance, the difference between the working electrode potential and the voltage being applied by the potentiostat also increases. This can be reduced by passing current through a counter electrode, rather than the reference, creating a 3-electrode cell. With little to no current flow between the reference and working electrode, the IR_S term can be minimized, and $E_{working}$ approaches E_{app}. While we do observe increasing gliosis over time in the postmortem histology, in our hands, the dominant electrode failure mode was the loss of the AgCl layer, and therefore loss of the reference's nonpolarizable character. In this case, we would not expect that diverting current flow through a counter electrode would mitigate reference polarization. We believe that this discrepancy in observed failure modes is due to the fact that FSCV measurements in the Seaton et al. study were performed *in vitro* using explanted electrodes, where adhered tissue may have been pulled out when the electrode was removed from the brain. Our group (Castagnola et al., 2020b) and others (Hashemi et al., 2011b) have previously observed significant differences in the electrochemical properties of explanted electrodes compared to *in vivo* electrodes. Additionally, the Ag/AgCl electrodes were constructed differently—soaked in sodium hypochlorite for 24 h in Seaton et al., compared to the faster electrochemical method used in this study. This may result in our electrodes having a thinner AgCl layer that was more easily stripped away over time. The electrodes used in this study were also significantly smaller than those used in Seaton et al. (127 vs 250 μm in diameter). This may have resulted in more significant gliosis in Seaton et al., leading to increased electrode impedance.

Ag/AgCl electrodes have been known for many years to be highly toxic (Dymond et al., 1970). Though it is well tolerated topically (Hadrup et al., 2018, 2021), and despite its desirable antibiotic effects, Ag has been abandoned as a material for the construction of implanted devices due to the tissue damage it causes, even in cases when it is not used as an electrode (Kraft et al., 2000). The mechanism of toxicity of Ag nanoparticles has been well studied, especially in aquatic environments (Bilberg et al., 2012; Dubey et al., 2015), but bulk Ag implants less so. Some potential mechanisms for damage caused by Ag implants include increased oxidative stress, DNA damage, and alteration of the activity of copper-dependent enzymes (Dubey et al., 2015). While the reference electrode—and therefore the damage caused by its implantation and toxicity—is typically far from the sensing site, the results of an experiment coupling electrochemical measurements to behavioral tasks may be swayed. A study from 1966 reported on the dangers of using Ag as an intra-cerebral electrode material after patients implanted with such electrodes developed abnormal EEG signals and serious cognitive impairments that persisted for several weeks after the electrodes were removed (Cooper and Crow, 1966). These patients did not have similar side effects from other metals, like gold or stainless steel. In our rats, immunohistochemistry performed at the site of the brain reference over the course of 3 weeks of implantation reveals increasing levels of apoptosis (caspase-3). While implantation itself could cause significant damage, such damage should start to settle down after 1–2 weeks. Instead, we saw increasing levels of cell death and GFAP reactivity suggesting the existence of persistent triggers, in agreement with the previous Ag toxicity report. Moving the reference electrode to an area outside of the brain and removing it when electrochemical sensing is not actively being performed will improve brain tissue health and prevent behavioral deficits caused by necrotic tissue distal from the working electrode site.

One of the main differences between the brain and subcutaneous references is the distance between the reference and the working electrode; in the subcutaneous case, the reference is several centimeters away

from the working electrode. Despite the increased distance, we saw no difference in impedance, background current, or DA oxidation potential between a fresh, brain-implanted reference and a fresh subcutaneous reference. This indicates that the increased distance between the reference and working electrodes in the case of the subcutaneous reference does not have a significant effect on the potential at the working electrode. Additionally, we had similar observations in data gathered from a mouse, in which both references are closer to the working electrode simply due to the size of the animal.

While we performed most of our measurements in anesthetized rats with the electrode inserted with a needle shuttle directly under the skin, a simple cannula system could easily be developed for ease of reference electrode placement, removal, and replacement in awake animals. While some studies have taken this approach (Saddoris et al., 2016), the electrode was still implanted into the brain. A subcutaneous cannula will likely minimize tissue damage and animal distress and therefore improve behavioral data quality.

Ag/AgCl electrodes are cheap and well characterized and are used in most *in vivo* sensing experiments due to their ease of construction and mechanical robustness. However, alternative reference electrode materials are beginning to be explored (Seaton and Heien, 2021). An essential requirement for reference electrodes—non-polarizability—rules out many electrode materials used for other applications, like stainless steel, gold, and platinum. Iridium oxide (IrOx) is one promising alternative to Ag/AgCl due to its biocompatibility, and has been used in sensing, stimulation, and recording studies *in vivo* (Li et al., 2009, 2016; Shi et al., 2021; Zheng et al., 2021). Unlike Ag/AgCl, IrOx is polarizable, although much less so than other electrode materials like platinum (Li et al., 2016). However, IrOx is highly sensitive to changes in pH (Seaton and Heien, 2021). While the brain pH is tightly controlled under normal circumstances, tissue damage can cause large changes in brain pH (De Salles et al., 1987; Siesjö, 1988). This may preclude the use of IrOx in experiments involving tissue damage, like stroke or traumatic brain injury models. Additionally, the effect of implantation damage-induced pH changes on IrOx has not been explored. Other electrode materials like boron-doped diamond (BDD) have also been utilized as a reference material (Seaton and Heien, 2021). However, while a study has used a BDD reference both for DA sensing *in vitro* as well as a reference for *in vivo* electrophysiological recording (Fan et al., 2020), to our knowledge, BDD has not yet been demonstrated as a sensing reference *in vivo*. That said, BDD has been shown to be biocompatible (Garrett et al., 2016; Hébert et al., 2014).

Here, we report a simple, effective way to prevent *in vivo* neurochemical sensing measurements from being affected by Ag/AgCl reference electrode polarization and toxicity. By moving the reference electrode to a subcutaneous implantation, a fresh electrode can be used during every recording session. There was no difference in impedance measured at a carbon fiber electrode using either a brain-implanted reference or a subcutaneous reference. We demonstrate that FSCV background signals and DA transient potential recorded with carbon fiber microelectrodes implanted for 3 weeks do not suffer from polarization-induced shifts with the use of a subcutaneous electrode. SEM/EDX reveals that Ag/AgCl electrodes implanted into the brain for 3 weeks have almost entirely lost their AgCl layer. Postmortem histology shows severe tissue damage at the brain implant site of the Ag/AgCl electrode, consistent with reports of the toxicity of Ag and AgCl implants. A subcutaneously implanted Ag/AgCl reference electrode will improve the accuracy of the applied potential compared to a chronically brain-implanted electrode, and has potential applicability to many chronic electrochemical sensing, drug release, and voltage transient experiments *in vivo*.

Limitation of the study

In this work, we only tested the effectiveness of the subcutaneous reference technique for three weeks following working electrode implantation and did not attempt to mitigate fouling of the carbon fiber electrode. We also did not analyze the tissue surrounding the subcutaneous reference to determine if there was any significant damage caused by the electrode. Because the electrode is only implanted for the duration of the measurement period and the tissue is only exposed to the electrode for a few hours at a time, we expect tissue damage around the subcutaneous to be minimal. However, this remains to be investigated. Additionally, we did not explore other reference electrode materials in this study.

STAR★METHODS

Detailed methods are provided in the online version of this paper and include the following:

- KEY RESOURCES TABLE

ACKNOWLEDGMENTS

This work was supported by the National Institutes of Health research grants R21DA049592, R21 NS123937, R01NS102725, and R01NS089688, and the National Science Foundation research grant # 1926756. Elaine Robbins is supported by National Institute of Neurological Disorders and Stroke T32 NS086749 Training Grant.

AUTHOR CONTRIBUTIONS

Conceptualization, E.C. and X.T.C.; Methodology, E.M.R. and E.C.; Investigation, E.M.R. and E.C.; Writing – Original Draft, E.M.R.; Writing – Review and Editing, E.M.R., E.C., and X.T.C.; Funding Acquisition, X.T.C.; Resources, X.T.C.; Supervision, X.T.C.

DECLARATION OF INTERESTS

The authors declare no competing interests.

Received: November 25, 2021
Revised: June 16, 2022
Accepted: July 22, 2022
Published: August 19, 2022

REFERENCES

Aoki, K. (1993). Theory of ultramicroelectrodes. Electroanalysis *5*, 627–639.

Atcherley, C.W., Laude, N.D., Parent, K.L., and Heien, M.L. (2013). Fast-scan controlled-adsorption voltammetry for the quantification of absolute concentrations and adsorption dynamics. Langmuir *29*, 14885–14892.

Bard, A.J., and Faulkner, L.R. (2001). Electrochemical Methods: Fundamentals and Applications (John Wiley & Sons, Inc).

Bilberg, K., Hovgaard, M.B., Besenbacher, F., and Baatrup, E. (2012). In vivo toxicity of silver nanoparticles and silver ions in zebrafish (Danio rerio). J. Toxicol. 293784. https://doi.org/10.1155/2012/293784.

Borgus, J.R., Puthongkham, P., and Venton, B.J. (2020). Complex sex and estrous cycle differences in spontaneous transient adenosine. J. Neurochem. *153*, 216–229. https://doi.org/10.1111/jnc.14981.

Castagnola, E., Robbins, E.M., Woeppel, K.M., McGuier, M., Golabchi, A., Taylor, I.M., Michael, A.C., and Cui, X.T. (2020a). Real-time fast scan cyclic voltammetry detection and quantification of exogenously administered melatonin in mice brain. Front. Bioeng. Biotechnol. *8*, 602216–602313. https://doi.org/10.3389/fbioe.2020.602216.

Castagnola, E., Woeppel, K., Golabchi, A., McGuier, M., Chodapaneedi, N., Metro, J., Taylor, I.M., and Cui, X.T. (2020b). Electrochemical detection of exogenously administered melatonin in the brain. Analyst *145*, 2612–2620. https://doi.org/10.1039/d0an00051e.

Cooper, R., and Crow, H.J. (1966). Toxic effects of intra-cerebral electrodes. Med. Biol. Eng. *4*, 575–581. https://doi.org/10.1007/BF02474827.

De Salles, A.A., Muizelaar, J.P., and Young, H.F. (1987). Hyperglycemia, cerebrospinal fluid Lactic acidosis, and cerebral blood flow in severely head-injured patients. Neurosurgery *21*, 45–50.

Dubey, P., Matai, I., Kumar, S.U., Sachdev, A., Bhushan, B., and Gopinath, P. (2015). Perturbation of cellular mechanistic system by silver nanoparticle toxicity: cytotoxic, genotoxic and epigenetic potentials. Adv. Colloid Interface Sci. *221*, 4–21. https://doi.org/10.1016/j.cis.2015.02.007.

Dymond, A.M., Kaechele, L.E., Jurist, J.M., and Crandall, P.H. (1970). Brain tissue reaction to some chronically implanted metals. J. Neurosurg. *33*, 574–580. https://doi.org/10.3171/jns.1970.33.5.0574.

Fan, B., Rusinek, C.A., Thompson, C.H., Setien, M., Guo, Y., Rechenberg, R., Gong, Y., Weber, A.J., Becker, M.F., Purcell, E., and Li, W. (2020). Flexible, diamond-based microelectrodes fabricated using the diamond growth side for neural sensing. Microsyst. Nanoeng. *6*, 1–12. https://doi.org/10.1038/s41378-020-0155-1.

Garrett, D.J., Saunders, A.L., McGowan, C., Specks, J., Ganesan, K., Meffin, H., Williams, R.A., and Nayagam, D.A.X. (2016). In vivo biocompatibility of boron doped and nitrogen included conductive-diamond for use in medical implants. J. Biomed. Mater. Res. B Appl. Biomater. *104*, 19–26. https://doi.org/10.1002/jbm.b.33331.

George, B.E., Barth, S.H., Kuiper, L.B., Holleran, K.M., Lacy, R.T., Raab-Graham, K.F., and Jones, S.R. (2021). Enhanced heroin self-administration and distinct dopamine adaptations in female rats. Neuropsychopharmacology *46*, 1724–1733. https://doi.org/10.1038/s41386-021-01035-0.

Hadrup, N., Sharma, A.K., Jacobsen, N.R., and Loeschner, K. (2021). Distribution, metabolism, excretion, and toxicity of implanted silver: a review. Drug Chem. Toxicol. 1–10. https://doi.org/10.1080/01480545.2021.1950167.

Hadrup, N., Sharma, A.K., and Loeschner, K. (2018). Toxicity of silver ions, metallic silver, and silver nanoparticle materials after in vivo dermal and mucosal surface exposure: a review. Regul. Toxicol. Pharmacol. *98*, 257–267. https://doi.org/10.1016/j.yrtph.2018.08.007.

Hashemi, P., Dankoski, E.C., Wood, K.M., Ambrose, R.E., and Wightman, R.M. (2011a). In vivo electrochemical evidence for simultaneous 5-HT and histamine release in the rat substantia nigra pars reticulata following medial forebrain bundle stimulation. J. Neurochem. *118*, 749–759. https://doi.org/10.1111/j.1471-4159.2011.07352.x.

Hashemi, P., Walsh, P.L., Guillot, T.S., Gras-Najjar, J., Takmakov, P., Crews, F.T., and Wightman, R.M. (2011b). Chronically implanted, nafion-coated Ag/AgCl reference electrodes for neurochemical applications. ACS Chem. Neurosci. *2*, 658–666. https://doi.org/10.1021/cn2000684.

He, C., Tao, M., Zhang, C., He, Y., Xu, W., Liu, Y., and Zhu, W. (2020). Microelectrode-Based electrochemical sensing technology for in vivo detection of dopamine: recent developments and future prospects. Crit. Rev. Anal. Chem. *52*, 544–554. https://doi.org/10.1080/10408347.2020.1811946.

Hébert, C., Scorsone, E., Bendali, A., Kiran, R., Cottance, M., Girard, H.A., Degardin, J., Dubus, E., Lissorgues, G., Rousseau, L., et al. (2014). Boron doped diamond biotechnology: from sensors to neurointerfaces. Faraday Discuss *172*, 47–59. https://doi.org/10.1039/c4fd00040d.

Heien, M.L.A.V., Khan, A.S., Ariansen, J.L., Cheer, J.F., Phillips, P.E.M., Wassum, K.M., and Wightman, R.M. (2005). Real-time measurement of dopamine fluctuations after cocaine in the brain of behaving rats. Proc. Natl. Acad. Sci. USA *102*, 10023–10028. https://doi.org/10.1073/pnas.0504657102.

Heien, M.L.A.V., Phillips, P.E.M., Stuber, G.D., Seipel, A.T., and Wightman, R.M. (2003). Overoxidation of carbon-fiber microelectrodes enhances dopamine adsorption and increases sensitivity. Analyst *128*, 1413–1419. https://doi.org/10.1039/b307024g.

Heinze, J. (1993). Ultramicroelectrodes in Electrochemistry. Angew. Chemie - Int. Ed. *32*, 1268–1288.

Hensley, A.L., Colley, A.R., and Ross, A.E. (2018). Real-time detection of melatonin using fast-scan cyclic voltammetry. Anal. Chem. *90*, 8642–8650. https://doi.org/10.1021/acs.analchem.8b01976.

Hoffman, A.F., Spivak, C.E., and Lupica, C.R. (2016). Enhanced dopamine release by dopamine transport inhibitors described by a restricted diffusion model and fast-scan cyclic voltammetry. ACS Chem. Neurosci. *7*, 700–709. https://doi.org/10.1021/acschemneuro.5b00277.

Howe, M.W., Tierney, P.L., Sandberg, S.G., Phillips, P.E.M., and Graybiel, A.M. (2013). Prolonged dopamine signalling in striatum signals proximity and value of distant rewards. Nature *500*, 575–579. https://doi.org/10.1038/nature12475.

Jackson, W.F., and Duling, B.R. (1983). Toxic effects of silver-silver chloride electrodes on vascular smooth muscle. Circ. Res. *53*, 105–108. https://doi.org/10.1161/01.RES.53.1.105.

Kahlert, H. (2010). Electroanalytical methods: guide to experiments and applications. In Electroanalytical Methods: Guide to Experiments and Applications, pp. 1–359. https://doi.org/10.1007/978-3-642-02915-8.

Kraft, C.N., Hansis, M., Arens, S., Menger, M.D., and Vollmar, B. (2000). Striated muscle microvascular response to silver implants: a comparative in vivo study with titanium and stainless steel. J. Biomed. Mater. Res. *49*, 192–199. https://doi.org/10.1002/(SICI)1097-4636(200002)49:2<192::AID-JBM6>3.0.CO;2-C.

Li, C., Ahn, C.H., Shutter, L.A., and Narayan, R.K. (2009). Toward real-time continuous brain glucose and oxygen monitoring with a smart catheter. Biosens. Bioelectron. *25*, 173–178. https://doi.org/10.1016/j.bios.2009.06.032.

Li, C., Limnuson, K., Wu, Z., Amin, A., Narayan, A., Golanov, E.V., Ahn, C.H., Hartings, J.A., and Narayan, R.K. (2016). Single probe for real-time simultaneous monitoring of neurochemistry and direct-current electrocorticography. Biosens. Bioelectron. *77*, 62–68. https://doi.org/10.1016/j.bios.2015.09.021.

Merrill, D.R., Bikson, M., and Jefferys, J.G.R. (2005). Electrical stimulation of excitable tissue: design of efficacious and safe protocols. J. Neurosci. Methods *141*, 171–198. https://doi.org/10.1016/j.jneumeth.2004.10.020.

Moatti-Sirat, D., Capron, F., Poitout, V., Reach, G., Bindra, D.S., Zhang, Y., Wilson, G.S., and Thévenot, D.R. (1992). Towards continuous glucose monitoring: in vivo evaluation of a miniaturized glucose sensor implanted for several days in rat subcutaneous tissue. Diabetologia *35*, 224–230.

Montague, P.R., McClure, S.M., Baldwin, P.R., Phillips, P.E.M., Budygin, E.A., Stuber, G.D., Kilpatrick, M.R., and Wightman, R.M. (2004). Dynamic gain control of dopamine delivery in freely moving animals. J. Neurosci. *24*, 1754–1759. https://doi.org/10.1523/JNEUROSCI.4279-03.2004.

Moran, R.J., Kishida, K.T., Lohrenz, T., Saez, I., Laxton, A.W., Witcher, M.R., Tatter, S.B., Ellis, T.L., Phillips, P.E., Dayan, P., and Montague, P.R. (2018). The protective action encoding of serotonin transients in the human brain. Neuropsychopharmacology *43*, 1425–1435. https://doi.org/10.1038/npp.2017.304.

Moussy, F., and Harrison, D.J. (1994). Prevention of the rapid degradation of subcutaneously implanted Ag/AgCl reference electrodes using polymer coatings. Anal. Chem. *66*, 674–679. https://doi.org/10.1021/ac00077a015.

Owesson-White, C., Belle, A.M., Herr, N.R., Peele, J.L., Gowrishankar, P., Carelli, R.M., and Wightman, R.M. (2016). Cue-evoked dopamine release rapidly modulates D2 neurons in the nucleus accumbens during motivated behavior. J. Neurosci. *36*, 6011–6021. https://doi.org/10.1523/JNEUROSCI.0393-16.2016.

Park, C., Oh, Y., Shin, H., Kim, J., Kang, Y., Sim, J., Cho, H.U., Lee, H.K., Jung, S.J., Blaha, C.D., et al. (2018). Fast cyclic square-wave voltammetry to enhance neurotransmitter selectivity and sensitivity. Anal. Chem. *90*, 13348–13355. https://doi.org/10.1021/acs.analchem.8b02920.

Park, J., Bucher, E.S., Budygin, E.A., and Wightman, R.M. (2015). Norepinephrine and dopamine transmission in 2 limbic regions differentially respond to acute noxious stimulation. Pain *156*, 318–327.

Patel, P.R., Na, K., Zhang, H., Kozai, T.D.Y., Kotov, N.A., Yoon, E., and Chestek, C.A. (2015). Insertion of linear 8.4 μm diameter 16 channel carbon fiber electrode arrays for single unit recordings. J. Neural. Eng. *12*, 046009. https://doi.org/10.1088/1741-2560/12/4/046009.

Patel, P.R., Popov, P., Caldwell, C.M., Welle, E.J., Egert, D., Pettibone, J.R., Roossien, D.H., Becker, J.B., Berke, J.D., Chestek, C.A., and Cai, D. (2020). High density carbon fiber arrays for chronic electrophysiology, fast scan cyclic voltammetry, and correlative anatomy. J. Neural. Eng. *17*, 056029. https://doi.org/10.1016/j.snb.2007.07.003.

Patel, P.R., Zhang, H., Robbins, M.T., Nofar, J.B., Marshall, S.P., Kobylarek, M.J., Kozai, T.D.Y., Kotov, N.A., and Chestek, C.A. (2016). Chronic in vivo stability assessment of carbon fiber microelectrode arrays. J. Neural. Eng. *13*, 066002. https://doi.org/10.1088/1741-2560/13/6/066002.

Phillips, P.E.M., Stuber, G.D., Heien, M.L.A.V., Wightman, R.M., and Carelli, R.M. (2003). Subsecond dopamine release promotes cocaine seeking. Nature *422*, 614–618. https://doi.org/10.1038/nature01476.

Puthongkham, P., Lee, S.T., and Venton, B.J. (2019). Mechanism of histamine oxidation and electropolymerization at carbon electrodes. Anal. Chem. *91*, 8366–8373. https://doi.org/10.1021/acs.analchem.9b01178.

Puthongkham, P., and Venton, B.J. (2020). Recent advances in fast-scan cyclic voltammetry. Analyst *145*, 1087–1102. https://doi.org/10.1039/c9an01925a.

Rafi, H., and Zestos, A.G. (2021). Review—recent advances in FSCV detection of neurochemicals via waveform and carbon microelectrode modification. J. Electrochem. Soc. *168*, 057520.

Rodeberg, N.T., Sandberg, S.G., Johnson, J.A., Phillips, P.E.M., and Wightman, R.M. (2017). Hitchhiker's guide to voltammetry: acute and chronic electrodes for in vivo fast-scan cyclic voltammetry. ACS Chem. Neurosci. *8*, 221–234. https://doi.org/10.1021/acschemneuro.6b00393.

Ross, A.E., and Venton, B.J. (2014). Sawhorse waveform voltammetry for selective detection of adenosine, ATP, and hydrogen peroxide. Anal. Chem. *86*, 7486–7493. https://doi.org/10.1021/ac501229c.

Saddoris, M.P., Wang, X., Sugam, J.A., and Carelli, R.M. (2016). Cocaine self-administration experience induces pathological phasic accumbens dopamine signals and abnormal incentive behaviors in drug-abstinent rats. J. Neurosci. *36*, 235–250. https://doi.org/10.1523/JNEUROSCI.3468-15.2016.

Samaranayake, S., Abdalla, A., Robke, R., Nijhout, H.F., Reed, M.C., Best, J., and Hashemi, P. (2016). A voltammetric and mathematical analysis of histaminergic modulation of serotonin in the mouse hypothalamus. J. Neurochem. *138*, 374–383. https://doi.org/10.1111/jnc.13659.

Samaranayake, S., Abdalla, A., Robke, R., Wood, K.M., Zeqja, A., and Hashemi, P. (2015). In vivo histamine voltammetry in the mouse premammillary nucleus. Analyst *140*, 3759–3765. https://doi.org/10.1039/c5an00313j.

Sanford, A.L., Morton, S.W., Whitehouse, K.L., Oara, H.M., Lugo-Morales, L.Z., Roberts, J.G., and Sombers, L.A. (2010). Voltammetric detection of hydrogen peroxide at carbon fiber microelectrodes. Anal. Chem. *82*, 5205–5210. https://doi.org/10.1021/ac100536s.

Saylor, R.A., Hersey, M., West, A., Buchanan, A.M., Berger, S.N., Nijhout, H.F., Reed, M.C., Best, J., and Hashemi, P. (2019). In vivo hippocampal serotonin dynamics in male and female mice: determining effects of acute escitalopram using fast scan cyclic voltammetry. Front. Neurosci. *13*, 1–13. https://doi.org/10.3389/fnins.2019.00362.

Schwerdt, H.N., Kim, M., Karasan, E., Amemori, S., Homma, D., Shimazu, H., Yoshida, T., Langer, R., Graybiel, A.M., and Cima, M.J. (2017a). Subcellular electrode arrays for multisite recording of dopamine in vivo. In Proceedings of the IEEE International Conference on Micro Electro Mechanical Systems (MEMS) (IEEE), pp. 549–552. https://doi.org/10.1109/MEMSYS.2017.7863465.

Schwerdt, H.N., Shimazu, H., Amemori, K.I., Amemori, S., Tierney, P.L., Gibson, D.J., Hong, S., Yoshida, T., Langer, R., Cima, M.J., and Graybiel, A.M. (2017b). Long-term dopamine neurochemical monitoring in primates. Proc. Natl. Acad. Sci. USA *114*, 13260–13265. https://doi.org/10.1073/pnas.1713756114.

Seaton, B.T., and Heien, M.L. (2021). Biocompatible reference electrodes to enhance chronic electrochemical signal fidelity in vivo. Anal. Bioanal. Chem. *413*, 6689–6701. https://doi.org/10.1007/s00216-021-03640-w.

Seaton, B.T., Hill, D.F., Cowen, S.L., and Heien, M.L. (2020). Mitigating the effects of electrode biofouling-induced impedance for improved long-term electrochemical measurements in vivo. Anal. Chem. *92*, 6334–6340. https://doi.org/10.1021/acs.analchem.9b05194.

Shi, D., Dhawan, V., and Cui, X.T. (2021). Bio-integrative design of the neural tissue-device interface. Curr. Opin. Biotechnol. *72*, 54–61. https://doi.org/10.1016/j.copbio.2021.10.003.

Siciliano, C.A., Saha, K., Calipari, E.S., Fordahl, S.C., Chen, R., Khoshbouei, H., and Jones, S.R. (2018). Amphetamine reverses escalated cocaine intake via restoration of dopamine transporter conformation. J. Neurosci. *38*, 484–497. https://doi.org/10.1523/JNEUROSCI.2604-17.2017.

Siesjö, B.K. (1988). Acidosis and ischemic brain damage. Neurochem. Pathol. *9*, 31–88. https://doi.org/10.1007/BF03160355.

Suzuki, H., Hiratsuka, A., Sasaki, S., and Karube, I. (1998). Problems associated with the thin-film Ag/AgCl reference electrode and a novel structure with improved durability. Sensor. Actuator. B Chem. *46*, 104–113. https://doi.org/10.1016/S0925-4005(98)00043-4.

Swamy, B.E.K., and Venton, B.J. (2007). Subsecond detection of physiological adenosine concentrations using fast-scan cyclic voltammetry. Anal. Chem. *79*, 744–750. https://doi.org/10.1021/ac061820i.

Taylor, I.M., Du, Z., Bigelow, E.T., Eles, J.R., Horner, A.R., Catt, K.A., Weber, S.G., Jamieson, B.G., and Cui, X.T. (2017a). Aptamer-functionalized neural recording electrodes for the direct measurement of cocaine in vivo. J. Mater. Chem. B *5*, 2445–2458. https://doi.org/10.1039/C7TB00095B.

Mitch Taylor, I., Jaquins-Gerstl, A., Sesack, S.R., and Michael, A.C. (2012). Domain-dependent effects of DAT inhibition in the rat dorsal striatum. J. Neurochem. *122*, 283–294. https://doi.org/10.1111/j.1471-4159.2012.07774.x.

Taylor, I.M., Robbins, E.M., Catt, K.A., Cody, P.A., Happe, C.L., and Cui, X.T. (2017b). Enhanced dopamine detection sensitivity by PEDOT/graphene oxide coating on in vivo carbon fiber electrodes. Biosens. Bioelectron. *89*, 400–410. https://doi.org/10.1016/j.bios.2016.05.084.

Walters, S.H., Robbins, E.M., and Michael, A.C. (2016). The kinetic diversity of striatal dopamine: evidence from a novel protocol for voltammetry. ACS Chem. Neurosci. *7*, 662–667. https://doi.org/10.1021/acschemneuro.6b00020.

Walters, S.H., Robbins, E.M., and Michael, A.C. (2015). Modeling the kinetic diversity of dopamine in the dorsal striatum. ACS Chem. Neurosci. *6*, 1468–1475. https://doi.org/10.1021/acschemneuro.5b00128.

Wang, B., Yang, P., Ding, Y., Qi, H., Gao, Q., and Zhang, C. (2019). Improvement of the biocompatibility and potential stability of chronically implanted electrodes incorporating coating cell membranes. ACS Appl. Mater. Interfaces *11*, 8807–8817. https://doi.org/10.1021/acsami.8b20542.

Wang, Y., and Venton, B.J. (2019). Caffeine modulates spontaneous adenosine and oxygen changes during ischemia and reperfusion. ACS Chem. Neurosci. *10*, 1941–1949. https://doi.org/10.1021/acschemneuro.8b00251.

Wassum, K.M., Tolosa, V.M., Wang, J., Walker, E., Monbouquette, H.G., and Maidment, N.T. (2008). Silicon wafer-based platinum microelectrode array biosensor for near real-time measurement of glutamate in vivo. Sensors *8*, 5023–5036. https://doi.org/10.3390/s8085023.

Weaver, C.L., Larosa, J.M., Luo, X., and Cui, X.T. (2014). Electrically controlled drug delivery from graphene oxide nanocomposite films. ACS Nano *8*, 1834–1843. https://doi.org/10.1021/nn406223e.

Weese, M.E., Krevh, R.A., Li, Y., Alvarez, N.T., and Ross, A.E. (2019). Defect sites modulate fouling resistance on carbon-nanotube fiber electrodes. ACS Sens. *4*, 1001–1007. https://doi.org/10.1021/acssensors.9b00161.

Welle, E.J., Woods, J.E., Jiman, A.A., Richie, J.M., Bottorff, E.C., Ouyang, Z., Seymour, J.P., Patel, P.R., Bruns, T.M., and Chestek, C.A. (2021). Sharpened and mechanically robust carbon fiber electrode arrays for neural interfacing. bioRxiv, 1–18.

West, A., Best, J., Abdalla, A., Nijhout, H.F., Reed, M., and Hashemi, P. (2019). Voltammetric evidence for discrete serotonin circuits, linked to specific reuptake domains, in the mouse medial prefrontal cortex. Neurochem. Int. *123*, 50–58. https://doi.org/10.1016/j.neuint.2018.07.004.

Wilson, L.R., Panda, S., Schmidt, A.C., and Sombers, L.A. (2018). Selective and mechanically robust sensors for electrochemical measurements of real-time hydrogen peroxide dynamics in vivo. Anal. Chem. *90*, 888–895. https://doi.org/10.1021/acs.analchem.7b03770.

Yuen, J., Goyal, A., Rusheen, A.E., Kouzani, A.Z., Berk, M., Kim, J.H., Tye, S.J., Blaha, C.D., Bennet, K.E., Jang, D.P., et al. (2021). Cocaine-induced changes in tonic dopamine concentrations measured using multiple-cyclic square wave voltammetry in vivo. Front. Pharmacol. *12*, 1–10. https://doi.org/10.3389/fphar.2021.705254.

Zheng, X.S., Griffith, A.Y., Chang, E., Looker, M.J., Fisher, L.E., Clapsaddle, B., and Cui, X.T. (2020). Evaluation of a conducting elastomeric composite material for intramuscular electrode application. Acta Biomater. *103*, 81–91. https://doi.org/10.1016/j.actbio.2019.12.021.

Zheng, X.S., Yang, Q., Vazquez, A.L., and Tracy Cui, X. (2021). Imaging the efficiency of PEDOT/CNT and iridium oxide electrode coatings for microstimulation. Adv. Nanobiomed Res. *1*, 1–17. https://doi.org/10.1002/anbr.202000092.

Zhou, L., Hou, H., Wei, H., Yao, L., Sun, L., Yu, P., Su, B., and Mao, L. (2019). In vivo monitoring of oxygen in rat brain by carbon fiber microelectrode modified with antifouling nanoporous membrane. Anal. Chem. *91*, 3645–3651. https://doi.org/10.1021/acs.analchem.8b05658.

STAR★METHODS

KEY RESOURCES TABLE

REAGENT or RESOURCE	SOURCE	IDENTIFIER
Antibodies		
Mouse monoclonal NeuN	Millipore	RRID: AB_2298772
Rabbit polyclonal anti-Iba1	Wake Chemicals	RRID: AB_839504
Rabbit monoclonal caspase-3	Cell Signaling	RRID: AB_2341188
Chicken GFAP	Sigma	RRID: AB_177521
Chemicals, peptides, and recombinant proteins		
Carbon fiber	Cytec LLC	T650
Ag wire	Goodfellow	786000
Experimental models: Organisms/strains		
Rat: Male, Sprague-Dawley	Charles Rivers	250-350 g
Mouse: Male, C57Bl/6J	Jackson Laboratory	8-12 weeks, 22-35 g
Software and algorithms		
MATLAB	Mathworks	R2020a
GraphPad Prism	GraphPad Software	v9.0
Other		
EI400 potentiostat	Out of production	None
Autolab potentiostat	Metrohm	PGSTAT128N
Sigma Analytical FE-SEM	Zeiss	500VP
FluoView confocal fluorescent microscope	Olympus, Inc.	FV1000

RESOURCE AVAILABILITY

Lead contact

Further information and requests for resources and reagents should be directed to and will be fulfilled by the lead contact, Xinyan Tracy Cui (xic11@pitt.edu).

Materials availability

This study did not generate new unique reagents. All materials are from commercial sources.

Data and code availability

Original data is available from the lead contact. No original code was generated for this study. Any additional information required to reanalyze the data reported in this paper is available from the lead contact upon request.

EXPERIMENTAL MODEL AND SUBJECT DETAILS

All procedures involving animals were approved by the University of Pittsburgh Institutional Care and Use Committee. Male Sprague-Dawley rats (Charles Rivers Inc. Wilmington, MA, USA) were anesthetized with isoflurane (4% for initial induction, followed by 2.5% for maintenance). Rats were placed on a thermal blanket and the head was fixed in a stereotaxic frame. The skin was resected from the skull and holes were drilled over the striatum (AP +1.0 mm, ML 3.8 mm from bregma) and the medial forebrain bundle (MFB, AP -4.3 mm, ML 1.2 mm from bregma). Additional holes were drilled for the insertion of a Ag/AgCl reference electrode (0.005″ diameter wire, A-M Systems, coated with AgCl by amperometric deposition in 3M KCl at 4V for 3 min) and bone screws as both a counter electrode and as anchors for the chronically implanted animals. The subcutaneous Ag/AgCl reference electrode (constructed identically to the brain-implanted reference) was inserted under the skin into the fat pad on the back with the aid of a needle. The

dura was then removed, and a carbon fiber microelectrode was slowly lowered 5.0 mm below dura so that the entire sensing area was in the striatum. The stimulating electrode (MS303S/1, Plastics One, Roanoke, VA) was lowered into the ipsilateral MFB. Stimulations were periodically performed during the lowering procedure to determine the optimal DV location to produce maximal DA overflow.

For chronic preparations, the craniotomies were covered with Kwik-Sil (World Precision Instruments, Sarasota, FL) and the carbon fiber, Ag/AgCl reference, and stimulating electrode were cemented in place with UV curing cement (Henry Schein, Melville, NY, USA). The subcutaneous reference electrode was gently removed. The rats were then returned to their home cages with food and water available *ad libitum* on a 12/12 light/dark cycle. Weekly, the rats were re-anesthetized, placed on a thermal blanket, and a new reference electrode was inserted subcutaneously, and electrochemical measurements were performed. After the experiments were completed, rats were deeply anesthetized with a ketamine/xylene cocktail and perfused with PBS followed by 4% paraformaldehyde and their brains were removed.

To detect DA transients, a male mouse (C57BL/6J, 8–12 weeks, 22–35 g; Jackson Laboratory, Bar Harbor, ME, USA) was anesthetized, and the carbon fiber and Ag/AgCl electrodes were implanted with sterile procedure as in the rats. In addition, a rectangular stainless-steel chamber frame (#CF-10, Narishige International, USA) was bonded to the skull with UV curing cement along with the electrodes. Weekly, the mouse was re-anesthetized, its head was fixed onto a treadmill using the chamber frame, and a second, freshly prepared Ag/AgCl electrode was inserted under the skin. The mouse was then allowed to wake up and FSCV data was recorded for 30 minutes using each reference electrode.

METHOD DETAILS

Electrochemical procedures

Cylindrical carbon fiber microelectrodes were constructed by threading individual carbon fibers (7 μm diameter T650 fibers, Cytec LLC, Piedmont, SC, USA) through borosilicate capillary with the assistance of acetone. Capillaries were pulled to a sharp tip with a capillary puller (Narishige, Los Angeles, CA, USA) and sealed in place with Spurr epoxy (Sigma-Aldrich), which was cured in an oven at 70 °C for 8 hours. The exposed carbon fiber was then cut to a length of 400 μm and a nichrome wire was inserted to make an electrical connection to the potentiostat. Carbon fibers were soaked in isopropanol for 20 minutes prior to insertion.

FSCV measurements were performed with an EI400 potentiostat (out of production) using CV TarHeels software. For DA measurements, the potential was scanned at a frequency of 10 Hz from −0.4 V to 1.3 V, and back to −0.4 V vs Ag/AgCl at 400 V/s. Stimulations consisted of biphasic, 2 ms pulses at 3 V, delivered at 60 Hz for 3 s by a stimulus isolator (Neurolog 800, Digitimer, Letchworth Garden City, UK).

Impedance measurements were taken with an Autolab potentiostat (Metrohm, Herisau, Switzerland) with Nova 2.1.4 software. Impedance was measured from 10^5 to 0.1 Hz, with 10 frequencies recorded per decade using a sine wave oscillation and a 0.01 V RMS voltage. Data analysis was performed using MATLAB (Mathworks Inc.) and GraphPad Prism (GraphPad Software, San Diego, CA).

Analysis of explanted electrodes

Ag/AgCl reference electrodes were removed from the rats' brains after perfusion and analyzed with SEM/EDX using a Zeiss Sigma 500 VP Analytical FE-SEM with Oxford Microanalysis with a 10 keV acceleration voltage.

Immunohistochemistry

The removed brain tissue was cryoprotected using optimal cutting temperature compound (OCT, Tissue-Tek, Torrance CA), frozen, and sectioned. Tissue sections were hydrated in PBS and blocked with 10% normal goat serum. Following 45 min in 0.5% Triton X-100 in PBS, the sections were incubated overnight with primary antibodies for mouse monoclonal NeuN (Millipore, MAB377, 1:500), rabbit polyclonal anti-Iba1 (Wako Chemicals, 01919741, 1:500), rabbit monoclonal caspase-3 (Cell Signaling, 9661S, 1:500), chicken GFAP (Sigma, AB5541, 1:500) and DAPI. Sections were then rinsed three times for five minutes each with PBS and incubated for two hours with AlexaFluor488 (goat anti rabbit, 1:500), AlexaFluor568 (goat anti mouse 1:500), and AlexaFluor633 (goat anti chicken, 1:500), from ThermoFisher Scientific

(Waltham, Massachusetts, USA). Images were acquired with an Olympus FluoView 1000 confocal fluorescent microscope (Olympus, Inc., Tokyo, Japan) at the Center for Biologic Imaging at the University of Pittsburgh.

QUANTIFICATION AND STATISTICAL ANALYSIS

Statistical analysis was performed with GraphPad Prism (GraphPad Software, San Diego, CA). $p < 0.05$ was considered statistically significant. * = $p < 0.05$, ** = $p < 0.005$, *** = $p < 0.0005$, **** = $p < 0.00005$, and ns = no significance.